Available online at www.sciencedirect.com

SCIENCE DIRECT®

Journal of Nuclear Materials 326 (2004) 156–162

journal of nuclear materials

www.elsevier.com/locate/jnucmat

Study of lanthanum orthophosphates polymorphism, in view of actinide conditioning

B. Glorieux [a,*], M. Matecki [b], F. Fayon [c], J.P. Coutures [a], S. Palau [a], A. Douy [c], G. Peraudeau [b]

[a] *Institut des Matériaux et Procédés, IMP-CNRS, Tecnosud, 66100 Perpignan, France*
[b] *Institut des Matériaux et Procédés, IMP-CNRS, Four Solaire, 66125 Font-Romeu, France*
[c] *Centre de Recherche sur les Matériaux à Haute Température, CRMHT-CNRS, 45071 Orléans, France*

Received 1 July 2003; accepted 6 January 2004

Abstract

In order to perform researches on the substitution lanthanide–actinide in a view of actinide conditioning, a preliminary study of the polymorphism of lanthanum orthophosphates has been carried out by different techniques. $LaPO_4$ formed by reaction of lanthanum nitrate with phosphoric acid contains 0.5 mol of water in open channel of the hexagonal structure (rhabdophane-type). The combination of thermogravimetric analysis, differential scanning calorimetry, X-ray diffraction and ^{31}P solid-state nuclear magnetic resonance clearly shows the different steps of the thermal treatment. The zeolitic water evaporates between 180 and 280 °C. After heating up to 700 °C, a monoclinic structure (monazite-type) is formed by compacting the chains of PO_4 tetrahedron alternating with LaO_9 polyhedron.

1. Introduction

Resurgent interest of ceramics matrix as material host for high level nuclear waste has induced new researches on materials that are able to store specific fission products or minor actinides [1]. The global purpose of these studies is to develop new matrix with improved physico-chemical durability for the storage of specific long live radioactive waste, compared to the so-called R_7T_7 glass. Lanthanides orthophosphate $LnPO_4$, with a monazite type structure, is one of these materials [2].

Bois [3] and Oelkers [4] have characterized the chemical durability of $LaPO_4$ using lixiviation tests and they have shown that monazite-type ceramics are highly resistant to the leaching process.

The potentiality of using monazite as a storage matrix is coming from geological studies [5,6]. Geological researchers [7,8] have determined in monazite of different age that below 900 °C, the geological monazite is able to contain other atoms for million of years, the framework of the crystal being totally untouched, what is exactly one goal of the law 'Bataille' [9] which leads our work. This interest of monazite is confirmed by measurements of impurities in monazite contained in granite of England [10].

Before storing actinides in the monazite, it is important to assess its thermophysical and chemical properties. The goal of this paper is to define the different steps of the formation of the lanthanum monoclinic orthophosphate (monazite synthetic analogue) obtained by thermal treatment of the lanthanum hexagonal orthophosphate (rhabdophane synthetic analogue).

Different ways are available to synthesize monazite [11,12]: precipitation by mixing lanthanide nitrate with monoammonium phosphate in a pH controlled solution with a molar ratio Ln/P of 30, solid reaction between lanthanide sesquioxide with monoammonium phosphate at 800 °C, high temperature reaction between the two last components quickly melted in a solar furnace, liquid

---

[*] Corresponding author. Tel.: +33-4 68 68 22 69; fax: +33-4 68 68 22 13.
E-mail address: glorieux@univ-perp.fr (B. Glorieux).

0022-3115/$ - see front matter © 2004 Elsevier B.V. All rights reserved.
doi:10.1016/j.jnucmat.2004.01.005

reaction of lanthanum sesquioxide with phosphoric acid, reaction between dissolved nitric lanthanide with phosphoric acid [13]. The last way of synthesis leads to the formation of a hexagonal lanthanide orthophosphate including zeolitic water. The paste is heated overnight at 800 °C, what compacts the structure and transforms the hexagonal structure into a monoclinic one.

It could be interesting to synthesize the orthophosphate by a melting/solidification step. For this purpose, we study the congruency behavior of $LaPO_4$. Previous works are not optimistic because of the volatility of P_2O_5 [14]. A solar furnace is used to study the melting solidification process of $LaPO_4$. The solar furnace is a unique equipment to perform this study because of the quickness and the easiness to melt any kind of materials by focusing up to 15 000 times the solar beam on a 15 mm target. The powder sample is molten thermally in a solar furnace during different periods, then characterized.

2. Experimental

2.1. Synthesis

The hexagonal phase of lanthanum orthophosphate (rhabdophane analogue) has been obtained by mixing $La(NO_3)_3$ (Aldrich, 99.9%) and H_3PO_4 (Merck, 99%) aqueous solutions. As suggested by Lucas [13], we have used a La/P ratio of 2 for the selective synthesis of $LaPO_4$ according to the following reaction:

$$La(NO_3)_3 + H_3PO_4 \xrightarrow[H_2O]{} LaPO_4 \cdot xH_2O + 3HNO_3 \qquad (1)$$

After 3 days of magnetically stirring in a closed vessel at 80 °C, the obtained precipitate is filtrated and washed with deionized water and then dried at 100 °C overnight.

2.2. Thermal analyses

Thermogravimetric (TGA) and semi-quantitative differential thermal analyses are performed on a SETARAM Setsys Evolution apparatus allowing simultaneous weight and heat flow measurements. The experiments were preformed under air atmosphere using platinum crucible (66 mg of sample) at a heating rate of 3 degrees per minute. The temperature was measured with an S thermocouple (Pt/Pt.Rh 10%).

2.3. Powder X-ray diffraction

The X-ray diffraction powder pattern were obtained at room temperature on an automated Philips PW 1820 diffractometer using the Ni filtered Cu Kα ($\lambda = 1.54184$ Å) radiation. Patterns are compared to the PDF database using XPERT Philips software; the spectra are smoothed using reverse FFT routine and peaks are identified by a second derivative technique. Cell parameters are calculated using a Rietveld technique with FullProf software.

2.4. Solid-state NMR

The ^{31}P solid-state NMR experiments were carried out on a Bruker DSX 400 spectrometer operating at a Larmor frequency of 161.99 MHz with a 4 mm MAS probehead. The ^{31}P magic angle spinning (MAS) NMR spectra were recorded with a spinning frequency of 10 kHz using a single pulse acquisition ($\pi/10$) and a recycle delay of 20 s to prevent saturation. The $\{^1H\}$–^{31}P cross polarization MAS (CP-MAS) spectra were acquired at a 10 kHz spinning frequency with ^1H continuous wave decoupling using a ramped polarization transfer and contact time varying from 500 μs to 15 ms. The ^{31}P chemical shifts were referenced relative to 75% H_3PO_4 aqueous solution. The spectra are fitted by different Voight functions [15].

3. Results and discussion

3.1. Characterization of the final powder

The powder resulting from the reaction (1) is X-ray characterized at room temperature. The pattern is the first of Fig. 1. It corresponds exactly to the rhabdophane reference as 75–1881 on the PDF2 database referring the work of Mooney [16]. The Rietveld refinement reveals a hexagonal structure with space group symmetry $P6_222$ and $Z = 3$. The determined unit cell parameters are $a = 0.71073(8)$ nm and $c = 0.6494(1)$ nm, in good agreement with those reported in the literature [16]. This hexagonal structure is made of PO_4 tetrahedra and LaO_8 polyhedra linked together to form chains alternating PO_4 and LaO_8 polyhedra along the hexagonal axis. The chains are linked together by P–O–La bonds leaving an open channel along the hexagonal axis. The open channel has a minimum diameter of 0.34 nm and can contain from 0 to 1 mol of water molecules, according to the literature [17]. This water content was determined in the following from TGA experiment.

3.2. Thermogravimetric analysis

The TGA curve of the $LaPO_4$ sample obtained at a heating rate of 3 °C/min is shown in Fig. 2. Assuming that the evaporation of water is the only phenomenon responsible of a weight loss Δm, this quantity is converted in mole of water Δx by the relation $\Delta x = \Delta m * M_{LaPO_4}/(m_f * M_{H_2O})$, with $M_{LaPO_4} = 233.88\ g\,mol^{-1}$, m_f the final weight of the sample and $M_{H_2O} = 18\ g\,mol^{-1}$. This curve evidences a significant weight loss from room temperature up to about 280 °C occurring in two steps.

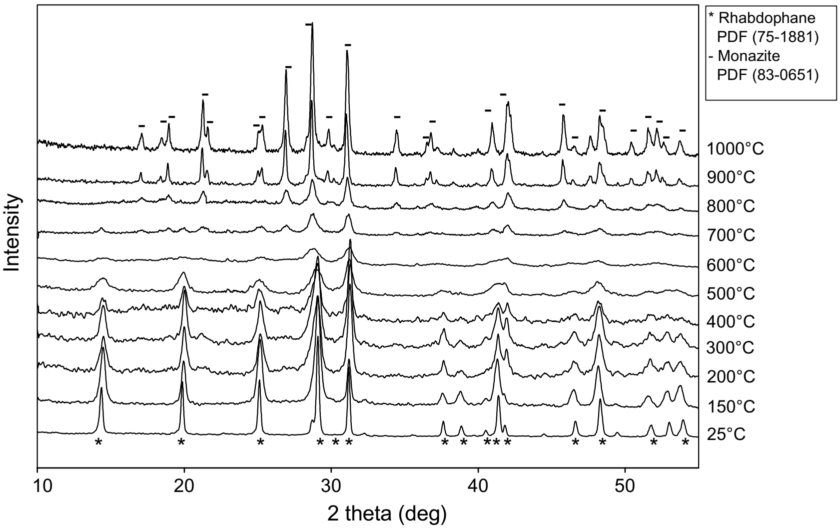

Fig. 1. XRD patterns of $LaPO_4$ heated at 3 °C/min, then cooled. Patterns are recorded at room temperature.

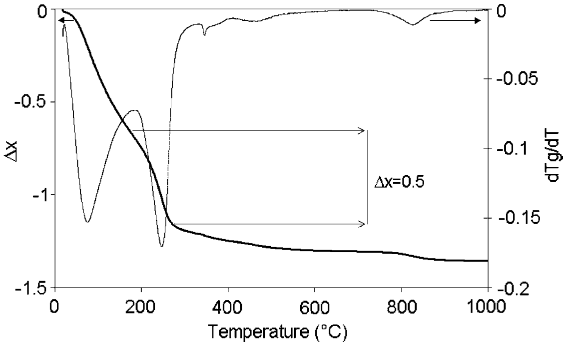

Fig. 2. Thermogravimetric analysis of $LaPO_4$ heated at 3 °C/min. $\Delta x = \Delta m * M_{LaPO_4}/(m_f * M_{H_2O})$, with Δm the weight loss, $M_{LaPO_4} = 233.88\ g\,mol^{-1}$, m_f the final weight of the sample and $M_{H_2O} = 18\ g\,mol^{-1}$.

The first step is from room temperature to 180 °C, while the second step is from 180 to 280 °C. The weight loss associated to this second step corresponds to 0.5 mol of water with an accuracy of 8%, suggesting that the stoichiometry of the sample is $LaPO_4 \cdot 0.5H_2O$. Those results are in agreement with the measurements of Nishihama et al. [18] and Ropp [19].

The weaker weight loss observed at higher temperature up to 450 °C might be mainly attributed to the evaporation of hydroxyl groups formed between hydrogen of water and oxygen of the PO_4 tetrahedron during reaction (1). Infrared spectroscopy would be interesting to detect the hydrogen configuration. The hydrogen atom might be link with oxygen of the PO_4 tetrahedron, or still in a water configuration.

The signal recorded during the cooling does not reveal any weight change.

3.3. Differential thermal analysis

The DSC trace of the $LaPO_4$ hexagonal phase for an heating rate of 3 °C/min is depicted in Fig. 3. Due to the S thermocouple, no information is extracted below 120 °C. The curve exhibits a first intense sharp endothermic peak located between 185 and 285 °C with an enthalpy of -91 ± 6 J/g and a second broader exothermic peak located between 590 and 740 °C with an enthalpy of 30 ± 2 J/g. The accuracy of the temperature measurement is about 8 °C. The first endothermic peak occurs during the weight loss detected by TGA and might certainly be associated to the evaporation of the zeolitic water contained in the hexagonal $LaPO_4$ structure, while

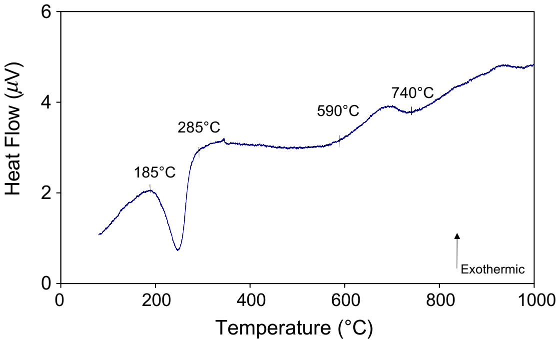

Fig. 3. Differential scanning calorimetry of $LaPO_4$ heated at 3 °C/min.

the second exothermic peak is attributed to the hexagonal–monoclinic structural phase transition.

That range of temperature is in agreement with the measurements of Jonasson et al. [20] but different than those of Nishihama et al. [18]: 890 °C, and those of Bondar et al. [21]: 400 °C. Regarding the literature data, this transition can occur from 400 °C, with a highly slow rate, to 900 °C, almost right away.

The DSC signal on cooling does not reveal any thermal event and suggests that the hexagonal–monoclinic transition is thermally irreversible.

These structural evolutions with temperature were characterized by powder X-ray diffraction and ^{31}P solid-state NMR.

3.4. Powder X-ray diffraction

The X-ray diffractions are performed at room temperature on sample heated at different temperatures ranging from 25 to 1000 °C (heating rate of 3 °C/min) then cooled. Patterns are depicted in Fig. 1. The pattern is similar to the one published by Ruigang et al. [12].

For heating between 100 and 400 °C, the XRD powder pattern remains characteristic of the $LaPO_4$ hexagonal structure. A small decrease of the unit cell parameters associated to a weak increase of the width of the reflection is observed as the temperature increases.

For the sample heated between 500 and 600 °C, a strong broadening of the hexagonal peaks is observed. After heating beyond the second exotherm observed in the DTA experiment (700 °C), the XRD powder pattern reveals the presence of the $LaPO_4$ monoclinic phase. At this temperature, two small and broad peaks at 14.5° and 20.0° (2θ) characteristic of the hexagonal phase are still observed. The XRD powder patterns of the samples heated at higher temperature (from 800 to 1000 °C) only evidence the $LaPO_4$ monoclinic phase with a monazite-type structure (space group $P2_1/n$, $Z = 4$). The unit cell parameters determined, with a Rietveld technique, for the sample heated at 900 °C are $a = 0.6836(6)$ nm, $b = 0.707(5)$ nm, $c = 0.6502(6)$ nm and $\beta = 103.27(4)$, in good agreement with previous work [11].

Measurements are performed on the same samples six months after those represented on Fig. 1. The patterns are totally unchanged.

This monoclinic structure is made of PO_4 tetrahedra and LaO_9 polyhedra linked together to from chains along the c axis resulting in a more compact organization than the hexagonal phase. According to Mooney [16] and Wyckoff [22], the average phosphor–oxygen and lanthanum–oxygen distances are respectively 0.15571 and 0.24878 nm in the rhabdophane structure and in the monazite structure respectively 0.15672 and 0.25349 nm, with an accuracy on the distances of about 1%. It means that the hexagonal–monoclinic transition, which consists to a compaction of the chain, implies an increase of the density of 20%, the insertion of one oxygen in the first shell of coordinance of the lanthanum and an increase of the La–O and P–O distances.

3.5. Solid-state NMR

In the following, the evolution of the ^{31}P local environment in $LaPO_4$ as a function of the temperature has been investigated using ^{31}P solid-state NMR spectroscopy. The NMR experiments are performed on the same samples than those analysed by X-ray diffraction.

The samples were transfer in a glove box just after the heating. The probehead were fill in the glove box as well.

The ^{31}P MAS spectra obtained for samples heated at different temperature are depicted in Fig. 4(a) and the fittings are shown in Table 1. The ^{1}H–^{31}P cross polarization MAS (CP-MAS) spectra, allowing the selective observation ^{31}P tetrahedral surrounded by ^{1}H nuclei, are displayed in Fig. 4(b). For example, four fittings are represented in Fig. 5.

As shown in these figures, the ^{31}P MAS NMR spectrum of the sample heated at 100 °C consists of a single resonance with a ^{31}P isotropic chemical shift of −3.35 ppm, characteristic of isolated PO_4^{3-} tetrahedra. This is in agreement with the $LaPO_4 \cdot 0.5H_2O$ structure, which contains a single crystallographic P site.

As expected for this hydrated compound, ^{31}P MAS and CP-MAS spectra obtained for various contact times remain almost similar until the dehydration process occurs. It should be mentioned that the MAS spectra of the sample heated to 150 and 200 °C display, in addition to the intense ^{31}P resonance of $LaPO_4 \cdot 0.5H_2O$, a weaker intensity peak located at about 1.6 ppm indicating the presence of a secondary phase. This phase contributes to less than 1% of the integrated intensity. Up to now, this phase, not observed by X-ray diffraction, is not attributed.

After heating up to 300 °C, a significant decrease of the signal intensity detected in the CP-MAS spectrum is observed. This CP-MAS spectrum shows two overlapping components at about −3.45 and −2.9 ppm. The ^{31}P resonance at −3.45 ppm corresponds to the ^{31}P sites neighbouring the residual water molecule contained in the $LaPO_4$ hexagonal structure, while the broad peak at −2.9 ppm could be attributed to HPO_4 groups formed during reaction (1). This broad component contributes to less than 5% of the integrated intensity in the quantitative MAS spectra and strongly overlaps with the intense ^{31}P resonance of $LaPO_4 \cdot 0.5H_2O$ in the CP-MAS spectra of samples heated at lower temperatures.

After heating up to 400 °C, the quantitative 1D MAS spectrum is mainly characteristic of the dehydrated $LaPO_4$ hexagonal phase and the ^{31}P CP-MAS spectrum only shows a broad peak of weak intensity attributed to

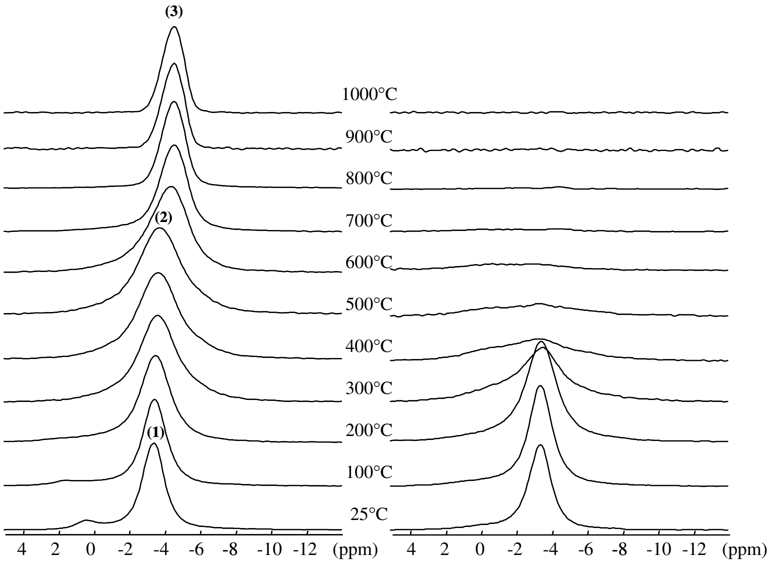

(a): ^{31}P MAS (b): ^{1}H-^{31}P VACP MAS

Fig. 4. (a) NMR ^{31}P MAS spectra and (b) ^{1}H–^{31}P VACP MAS in $LaPO_4$.

Table 1
Deconvolution of the NMR ^{31}P spectra of $LaPO_4$

T (°C)	$LaPO_4 \cdot 0.5H_2O$ hexagonal (#1)			$LaPO_4$ hexagonal (#2)			$LaPO_4$ monoclinic (#3)		
	δiso	FWHM	I	δiso	FWHM	I	δiso	FWHM	I
25	−3.35	1.5	100						
100	−3.4	1.6	100						
200	−3.4	2.0	86	−3.65	2.6	14			
300	−3.45	2.92	20	−3.65	2.6	80			
400	−3.42	4	14	−3.65	2.7	86			
500	−3.42	4.2	9	−3.75	2.9	91			
600	−3.4	3.56	4	−3.8	3	54	−4.5	1.9	42
700				−3.8	3.3	15	−4.5	1.8	85
800							−4.45	1.5	100
900							−4.45	1.4	100
1000							−4.45	1.4	100

the residual HPO_4 groups. As the temperature increases from 100 to 500 °C, the line width of the ^{31}P resonance assigned to the $LaPO_4$ hexagonal phases significantly increases (from 1.5 to 2.9 ppm), indicating an increase of the distribution of the PO_4 tetrahedron local environments in the structure. A significant broadening of the reflections observed in XRD powder patterns also evidences this increase of the local disorder.

After heating up 600 and 700 °C, a significant modification of the MAS spectrum, reflecting the hexagonal–monoclinic phase transition is observed. These spectra were simulated with two components at −3.8 and −4.5 ppm, assigned to the ^{31}P resonances of the hexagonal and monoclinic $LaPO_4$ phases, respectively.

For the samples heated to higher temperatures, the MAS spectra evidence the single ^{31}P resonance, located at −4.5 ppm, expected from the $LaPO_4$ monoclinic structure. The width of the peak decrease with the temperature, meaning an increase of the order in the structure, which is also evidenced by the same phenomenon in XRD powder patterns.

A quantitative comparison of the crystallinity between XRD and NMR is not reasonable because of the difference of the parameter measured in each technique (global structural ordering for XRD and local environment for NMR).

Important points were revealed by experiments where $LaPO_4$ was pounded in an open room. The cross

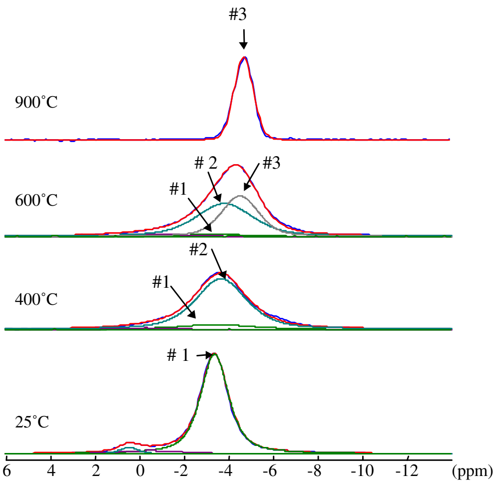

Fig. 5. Fittings of the NMR ^{31}P MAS spectra.

polarization measurements were not clear, quantity of phosphorous surrounded by hydrogen seems randomized. It appears that, due to the thermal and mechanical effects produced by the grinding, water molecules can easily be reabsorbed by the hexagonal structure in the open channel.

3.6. Congruency study

The study of the congruency of $LaPO_4$ is performed in order to explore the ability of $LaPO_4$ to be prepared by a process using a melting step. In this perspective, we melted 1 g of monoclinic $LaPO_4$ during different period of time. Solar furnace [23] is adjusted to focus 2 kW with a concave mirror on a 15 mm diameter target. Final samples are characterized by X-ray diffraction shown on Fig. 6. A study of the weight lost during the melting is difficult because of the important lost of sample due to the thermal shock.

During the first second of melting, $LaPO_4$ is still present, but with change in crystallinity. Small peaks appearing at 22.85°, 37.7° and 45.3° are not understood for the moment. After a melting of 30 s, $La_7P_3O_{18}$ and αLa_3PO_7 start appearing. That means a loss of P_2O_5 molecules by volatilization in the $LaPO_4$ and the $La_7P_3O_{18}$ structures. According to the phase diagram rules and because La_2O_3 is not identified in the pattern, $LaPO_4$ and $La_7P_3O_{18}$ have a non congruent melting behavior and La_3PO_7 may present a congruency melting.

4. Conclusion

An extensive study has been performed on lanthanum orthophosphates polymorphism. Rhabdophane-type samples are synthesized by mixing lanthanide nitrate with phosphoric acid. The samples are thermally treated and characterized using TGA, DSC, XRD and NMR. The different phenomena taking place during the thermal treatment at 3 °C/min following by a quenching are characterized:

- evaporation of water, from room temperature to 180 °C, this water being probably superficial water,
- evaporation of water stored in open channel of the rhabdophane-type structure between 180 and 280 °C, this water being probably zeolitic water,
- crystallinity lost of the hexagonal phase up to 600 °C, to obtain at this temperature a poorly crystallized state of the structure,
- transformation of the hexagonal phase in the monoclinic phase from 600 to 800 °C,
- crystallinity increase of the monoclinic phase from 800 to 1000 °C.

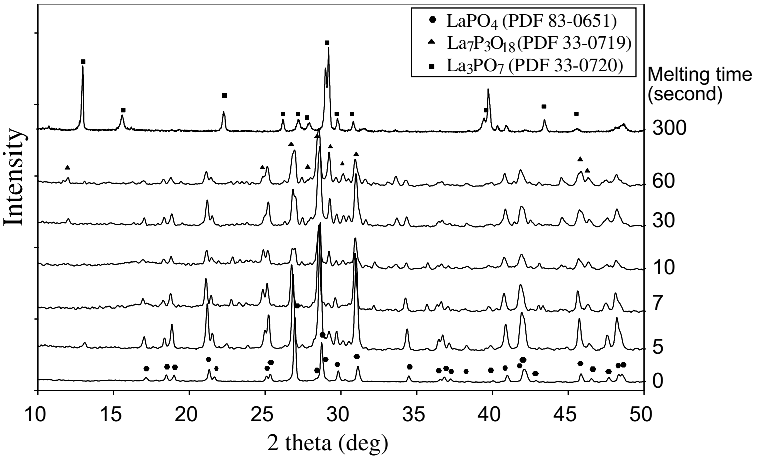

Fig. 6. XRD patterns of monoclinic $LaPO_4$ molten in a solar furnace during different period of times.

An important point not mentioned by the literature but clearly evidenced by this work is the existence of a dry lanthanum orthophosphate in a hexagonal structure. This structure is not stable and can easily reabsorb water.

Because the structure of the orthophosphate changes during a melting process into a La_3PO_7 structure, an important structural study combined with lixiviation experiment of La_3PO_7 should be interesting in view of developing a synthesis of $LaPO_4$ by melting.

Acknowledgements

This work is supported in the frame of the research program NOMADE (GDR 2023) funded by the CNRS.

The authors thanks René Berjoan for several precious discussions, François Sibieude for his crystallographic knowledge, Eric Beche for his teaching of all the diffraction set-up and Christine Picard for her help in the TGA experiments.

References

[1] R.C. Ewing, W.J. Weber, F.W. Clinard, Prog. Nucl. Energy 29 (1995) 63.
[2] Y. Hikichi, O. Toshitaka, T. Hattori, Mineral. J. 19 (1997) 123.
[3] L. Bois, M.J. Guittet, F. Carrot, P. Trocellier, M. Gautier-Soyer, J. Nucl. Mater. 297 (2001) 129.
[4] E.H. Oelkers, F. Poitrasson, Chem. Geol. 191 (2002) 73.
[5] I. Braun, J.M. Montel, C. Nicollet, Chem. Geol. 146 (1998) 65.
[6] J.M. Montel, S. Foret, M. Veschambre, C. Nicollet, A. Provost, Chem. Geol. 131 (1996) 37.
[7] J.M. Montel, J. Kornprobst, D. Vielzeuf, J. Metamorph. Geol. 18 (2000) 335.
[8] S. Teufel, W. Heinrich, Chem. Geol. 137 (1997) 273.
[9] Loi 91-1381, Journal Officiel, Dec. 30, 1991, Fr.
[10] F. Poitrasson, S. Chenery, D.J. Bland, Earth. Planet. Sci. Lett. 145 (1996) 79.
[11] J.J. Serra, J. Coutures, A. Rouanet, H. Dexpert, Rev. Int. Hautes. Temp. Refr. Fr. 15 (1978) 287.
[12] W. Ruigang, P. Wei, C. Jian, F. Minghao, C. Zhenzhu, L. Yongming, Mater. Chem. Phys. 79 (2003) 30.
[13] S. Lucas, E. Champion, C. Penot, G. Leroy, D. Bernache-Assollant, Key Eng. Mater. 206 (2002) 47.
[14] J.J. Serra, J. Coutures, A. Rouanet, High Temp.–High Pres. 8 (1976) 337.
[15] D. Massiot, D. Fayon, M. Capron, I. King, Magn. Reson. Chem. 40 (2002) 70.
[16] R.C.L. Mooney, Acta Crystallogr. 3 (1950) 337.
[17] H. Assaaoudi, A. Ennaciri, A. Rulmont, M. Harcharras, Phase Transition 72 (2000) 1.
[18] S. Nishihama, T. Hirai, I. Komasawa, J. Mater. Chem. 12 (2002) 1053.
[19] R.C. Ropp, J. Electrochem. Soc. 115 (1968) 841.
[20] R.G. Jonasson, E.R. Vance, Thermochim. Acta 108 (1986) 65.
[21] I.A. Bondar, A.I. Domanskii, L.P. Mezentseva, M.G. Degen, N.E. Kalinina, Russ. J. Inorg. Chem. 21 (1976) 1126.
[22] R.W.G. Wyckoff, Crystal Struct. 3 (1963) 33.
[23] D. Laplaze, D. Bernier, G. Flamant, M. Lebrun, Synth. Met. 77 (1996) 67.